Inorganic Chemistry

Article

pubs.acs.org/IC

Bonding Study on the Chemical Separation of Am(III) from Eu(III) by S-, N-, and O-Donor Ligands by Means of All-Electron ZORA-DFT Calculation

Masashi Kaneko,[†] Sunao Miyashita,[†] and Satoru Nakashima*[,†,‡]

[†]Department of Chemistry, Graduate School of Science and [‡]Natural Science Center for Basic Research and Development, Hiroshima University, 1-3-1 Kagamiyama, Higashi-Hiroshima, Hiroshima 739-8526, Japan

Supporting Information

ABSTRACT: We performed a theoretical investigation for the selectivity of Eu(III)/Am(III) ions depending on the donor atoms by means of all-electron ZORA-DFT calculation. We estimated their selectivity as the relative stability in the complex formation reaction. The B2PLYP functional reproduced the experimental selectivity in which S- and N-donor ligands favor Am(III) ion, but O-donor ligand favors Eu(III) ion. Mulliken's bond overlap population analysis revealed that the contribution of the f orbital to the bonding was small or zero for Eu complex, whereas it was large for Am complex. The bonding nature of the f orbital for Am ion was the bonding type to S- and N-donor ligands, while it was the antibonding type to O-donor ligand. It was suggested that the difference in the bonding nature between the f orbital in the metal and the donor atoms determines the selectivity of Eu(III)/Am(III) by donor ligands.

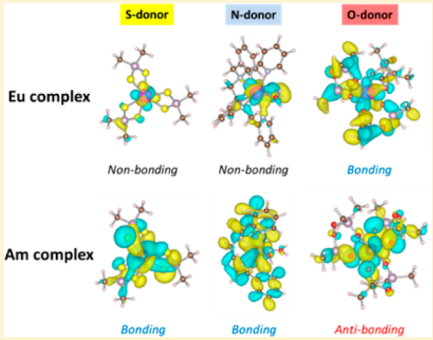

1. INTRODUCTION

The separation study of minor actinides (MA), which include Am and Cm, from lanthanides (Ln) is important for the partitioning and transmutation (P&T) strategy of MA from radioactive high-level liquid waste (HLLW), because MA ions have similar chemical properties to Ln ions in aqueous solution.[1] The solvent-extraction experiments have given useful results for the separation of Am(III) ion from Eu(III) ion. For example, bis(2,4,4-trimethylpentyl)dithiophosphinic acid (Cyanex-301) and *N*,*N*,*N*′,*N*′-tetrakis(2-pyridylmethyl)-ethylenediamine (TPEN) ligands, which behave as S- and N-donor ligands, respectively, favor Am(III) ion,[2,3] whereas bis(2,4,4-trimethylpentyl)phosphinic acid (Cyanex-272) as O-donor ligand favors Eu(III) ion[4] (Figure 1). These selective behaviors for the Eu(III)/Am(III) separation depending on the kind of donor atom of the ligands have been explained by the difference in the bonding properties of the f orbital between Eu(III) and Am(III) but are not still obvious.

Jensen and co-workers reported the extraction schema for Eu(III) and Am(III) ions with Cyanex-301 and Cyanex-272 ligands.[4] It was indicated that three equivalents of monomeric Cyanex-301 and dimeric Cyanex-272 coordinate to one metal ion.[4] EXAFS and UV−vis spectroscopic experiments have ensured these results and submitted geometrical data of the extracts of Sm(III) and Cm(III) ions whose coordination spheres are octahedral.[5] Watanabe and co-workers revealed that one equivalent of TPEN coordinates to one metal ion for Eu(III) and Am(III) systems.[3] Jensen et al. also suggested that the 1.8(5) molecules of water coordinate to the inner coordination sphere of $[Eu^{III}(TPEN)]^{3+}$ in aqueous solution, indicating that TPEN works as a hexadentate chelate,[6] because f-block compounds generally show a large coordination number of 8 or 9.

The computational study on lanthanide[7] and actinide[8] chemistries has been vital owing to the development of theoretical calculation procedures such as the development of relativistic Hamiltonian and basis function. The application of the computation to Ln/MA separation has been performed extensively.[9] Theoretical investigations of the complex formation process for Ln/MA ions with ligands have been employed for understanding the stability and selectivity of MA ion compared to Ln ion by various ligands. In research on the Cyanex-301 system, Cao et al. first performed the density functional calculation and indicated that the solvation effect, especially the hydration effect, is required to reproduce the selectivity of Eu(III)/Am(III) ions.[10] This consideration was supported by later work about not only other dithiophosphinic acid ligands[11,12] but also 6,6′-bis(1,2,4-triazin-3-yl)-2,2′-bipyridine (BTBP) ligand as N-donor chelate.[13] These results suggested that the relative stability in the complex formation reaction under aqueous solution determines the selectivity of Eu(III)/Am(III) separation, and the explicit consideration of the Gibbs energy difference between the hydration complex $[M(H_2O)_n]^{3+}$ and the extracted complex for each system is a key factor.

An investigation of the bonding nature in f-block compounds has been performed by means of relativistic DFT calculation. Kaltsoyannis estimated the covalency of $[An^{III}Cp_3]$[14] and $[An^{IV}Cp_4]$[15] (An = Th, Pa, U, Np, Pu, Am, and Cm;

Received: May 28, 2015
Published: July 9, 2015

DOI: 10.1021/acs.inorgchem.5b01204
Inorg. Chem. 2015, 54, 7103−7109

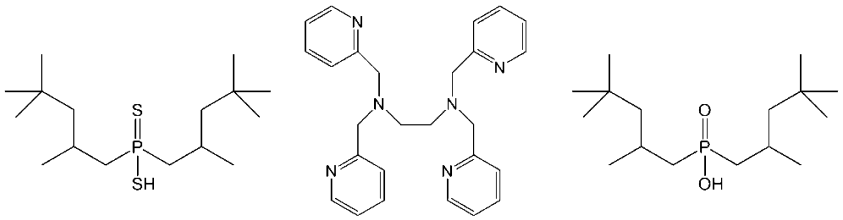

(a) Cyanex-301 **(S-donor)** (b) TPEN **(N-donor)** (c) Cyanex-272 **(O-donor)**

D_{Am}/D_{Eu} 5900[a] 100[b] 0.058[c]

Figure 1. Donor ligands and their separation factors of Am(III) ion from Eu(III) ion (D_{Am}/D_{Eu}) for (a) Cyanex-301 (ref 2), (b) TPEN (ref 3), and (c) Cyanex-272 (the value when the concentration of [Cyane-272] is $10^{-1.4}$ M in ref 4).

Cp = η^5-C_5H_5) by Mulliken's spin population and atoms-in-molecules analyses. Jensen and co-workers performed the bond overlap population analysis for $[M^{III}(bp18c6)]^+$ (M = Gd and Cm; H_2bp18c6 = *N*,*N*′-bis[(6-carboxy-2-pyridyl)methyl]-1,10-diaza-18-crown-3) and revealed the difference in the contribution of the f orbital between Gd and Cm complexes.[16] Recently, we estimated the validity of density functionals to reproduce the bonding property of f-block compounds by benchmarking between the experimental ^{151}Eu and ^{237}Np Mössbauer isomer shifts and scalar-relativistic ZORA DFT calculation.[17] As a result, we indicated that the performance of the reproducibility increases in the order of BP86, B3LYP, and B2PLYP functionals; in particular, B2PLYP results strongly correlate to experiments.

In this study, employing the above methods whose validity was ensured by benchmarking, we confirm the performance of all-electron ZORA-DFT calculation for the Eu(III)/Am(III) selectivity by Cyanex-301, TPEN, and Cyanex-272 ligands. The origin of its selectivity depending on ligands is investigated by population analyses to molecular orbitals such as spin population and bond overlap population. The bonding investigation of Eu(III) and Am(III) complexes with three kinds of donor atoms (S, N, and O) is the first attempt. We expect that a detailed understanding of Eu(III)/Am(III) selectivity depending on donor atoms leads one to predict the separation behavior and to design novel separation materials in which the effective functional group and donor atom are introduced.

2. COMPUTATIONAL DETAILS

As shown in Scheme 1, we consider the complex formation reaction from a hydrated metal complex. We set the hydration complex for both Eu and Am ions as $[M^{III}(H_2O)_9]^{3+}$, because the most stable oxidation state for them in solution is trivalent[18] and the reported primary hydration number of each aqua complex is 8.71[19] or 8.85[20] for Eu ion and 9.00[21] for Am ion. In all complexes, we assume the same reaction processes for both Eu and Am systems. As mentioned above, because the hydration number of the inner sphere of $[Eu^{III}(TPEN)]^{3+}$ was 1.8(5), we consider the TPEN complex as $[M^{III}(TPEN)(H_2O)_2]^{3+}$. The Gibbs energy ($G$) of each state is obtained by the following equations

Scheme 1. Complex Formation Reaction Schema for S-, N-, and O-Donor Systems

(a) Cyanex-301

$$[M(H_2O)_9]^{3+} + 3R_2PS_2^- \longrightarrow [M(R_2PS_2)_3]^0 + 9H_2O$$

(b) TPEN

$$[M(H_2O)_9]^{3+} + TPEN \longrightarrow [M(TPEN)(H_2O)_2]^{3+} + 7H_2O$$

(c) Cyanex-272

$$[M(H_2O)_9]^{3+} + 3(R_2PO_2)_2H^- \longrightarrow [M\{(R_2PO_2)_2H\}_3]^0 + 9H_2O$$

$$\Delta G = G_{final} - G_{initial} \quad (1)$$

$$G = E^{tot} + G^{corr} \quad (2)$$

$$G^{corr} = U^{corr} + k_BT - TS \quad (3)$$

$$U^{corr} = E^{ZPE} + E^{vib} + E^{rot} + E^{trans} \quad (4)$$

$$S = S^{spin} + S^{vib} + S^{rot} + S^{trans} \quad (5)$$

where E^{tot}, G^{corr}, U^{corr}, S, k_B, and T are the total energy, the thermal Gibbs correction term, the thermal correction term for inner energy, the entropy term, Boltzmann's constant, and temperature, respectively. The superscript words, ZPE, vib, rot, and trans, for U or S are the contributions of zero-point energy, vibration, rotation, and translation, respectively, to the inner energy or entropy terms.

Here, we mention the molecular structures employed for the present DFT calculation. For $[M^{III}(H_2O)_9]^{3+}$, we employ the single-crystal X-ray coordinates of tricapped trigonal complex $[M^{III}(H_2O)_9]$ $(CF_3SO_3)_3$ (M = Eu,[22] Am[23]). For $[M^{III}(R_2PS_2)_3]$, we refer to the X-ray coordinate of $[Sm^{III}(Cy_2PS_2)_3]$ (Cy = cyclohexyl) for both Eu and Am systems and replace the Cy group with a methyl group to reduce the computational cost.[24] For $[M^{III}(TPEN)(H_2O)_2]^{3+}$, we refer to the X-ray coordinates of $[Eu^{III}(TPEN')Cl_2]$ (ClO_4) (TPEN′ = *N*,*N*,*N*′,*N*′-tetrakis(2-pyridylmethyl)-(*R*)-propylenediamine) for both systems and replace two Cl atoms with two H_2O molecules.[25] For $[M^{III}\{(R_2PO_2)_2H\}_3]$, we construct the molecular geometry whose coordination sphere is octahedral based on the literature,[5] because its X-ray structure is not available. The metal ion is chelated by dimeric phosphinic acid bridged through the hydrogen bond, ←O═P(R_2)—O—H---O═P(R_2)—O$^-$→. We create this structure having pseudo-C_3 symmetry and calculate the R group as a methyl group similar to the dithiophosphinic complex.

All DFT calculations were performed using the program ORCA ver. 3.0.0[26] developed by Neese. The scalar-relativistic zero-order regular approximation (ZORA) Hamiltonian which includes the atomic model potential[27] and the perturbative treatment of the Breit−Pauli spin−orbit coupling term are employed to consider the relativistic effect. Segmented all-electron relativistic contracted (SARC) Gaussian-type basis sets are assigned to Eu ($61^{17}/51^{11}/41^8/41^2$)[28] and Am ($91^{20}/81^{12}/71^9/61^6$)[29] atoms for both optimization and single-point calculations. In geometry optimization, we employ the relativistic all-electron Gaussian basis sets TZV-ZORA[30] for P and S atoms and SV-ZORA[30] for H, C, N, and O atoms added to one polarization function. In the single-point calculation, we assign QZV-ZORA[30] with 2df polarization to S and P atoms, TZV-ZORA[30] with 2df polarization to C, N, and O atoms, and TZV-ZORA[30] with one polarization to the H atom. Geometry optimizations are performed by the quasi-Newton procedure at the ZORA-BP86 level without any geometrical

DOI: 10.1021/acs.inorgchem.5b01204
Inorg. Chem. 2015, 54, 7103−7109

constraints under gas-phase condition. Normal vibration modes are obtained under the strictly harmonic approximation at the BP86 level. Thermal correction for the Gibbs energy (G^{corr}) is calculated at 298.15 K and 1.00 atm. Single-point calculations are performed by three density functionals, BP86, B3LYP, which is the defined version in TurboMole program, and B2PLYP. We consider not only the total energy in the gas phase (E^{tot}_{gas}) but also that in aqueous phase (E^{tot}_{water}) obtained by self-consistent reaction field (SCRF) calculation with a conductor-like screening model (COSMO) set to a dielectric constant of 80.4 and refractive index of 1.33. The COSMO radii are assigned to 1.904 and 1.99 Å for Eu[31] and Am[32] atoms, respectively. Angular grid points in self-consistent field (SCF) calculations are set to Lebedev194 for optimization with no final grid calculation and Lebedev302/Lebedev434 for single-point calculation (iteration/final grid). Integral accuracy parameters are set to 4.34 for optimization and 4.67/5.01 for single-point calculation where the special grid is additionally constructed for Eu and Am atoms with an integral accuracy of 14.0 in order to improve the precision of SCF energies. All SCF calculations are achieved under the generally tight condition imposing a threshold value of 10^{-8} hartree to total energy difference during iteration. We employ the resolution of the identity (RI) approximation, Split-RI-J[33] for pure DFT and RIJCOSX[34] for hybrid DFT, for all SCF calculations under the unrestricted Kohn–Sham equation. The spin multiplet of Eu(III) and Am(III) complexes is set to spin septet. We obtain the spin population[35] and bond overlap population[36] by Mulliken's procedure. Three-dimensional descriptions of the optimized structures and molecular orbital spinors are visualized by using the program VESTA ver. 3.3.0.[37]

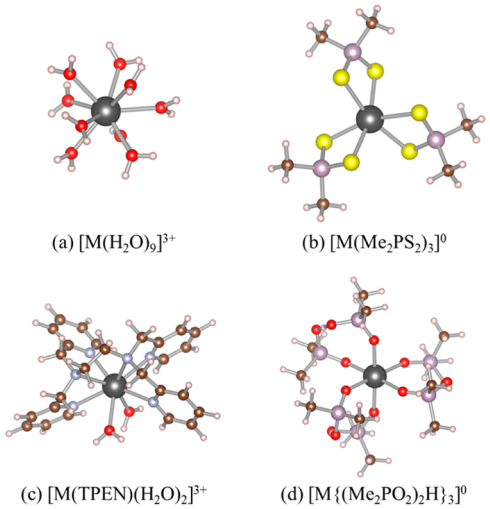

Figure 2. Three-dimensional geometries of optimized metal complexes for (a) $[M(H_2O)_9]^{3+}$, (b) $[M(Me_2PS_2)_3]^0$, (c) $[M(TPEN)(H_2O)_2]^{3+}$, and (d) $[M\{(Me_2PO_2)_2H\}_3]^0$. Black, yellow, purple, red, blue, brown, and light pink spheres show metal, S, P, O, N, C, and H elements, respectively.

3. RESULTS AND DISCUSSION

3.1. Geometry Optimization. All structures were converged without problems by geometry optimization and obtained with no imaginary frequencies for normal vibration mode calculation. Their Cartesian coordinates are shown in the Supporting Information (as .xyz file format). All Am(III) complexes had similar coordination geometries, including the bond lengths and bond angles between the metal and the ligands, to Eu(III) complexes. We show the equilibrium structures of metal complexes in Figure 2. The calculated geometries of $[M(H_2O)_9]^{3+}$, $[M(Me_2PS_2)_3]^0$, and $[M(TPEN)(H_2O)_2]^{3+}$ were obtained with a minor change compared to their reference structures. Pseudo C_3 symmetry was observed in $[M(H_2O)_9]^{3+}$, $[M(Me_2PS_2)_3]^0$, and $[M\{(Me_2PO_2)_2H\}_3]^0$ complexes. Table 1 shows the metal–ligand lengths of Eu and Am complexes. As a result, we indicate that the calculated bond lengths are in good agreement with the experiments within the deviation of 0.1 Å except those of M–P lengths for $[M\{(Me_2PO_2)_2H\}_3]^0$. The reason might be that the nine-membered ring containing metal and $(Me_2PO_2)_2H$ for $[M\{(Me_2PO_2)_2H\}_3]^0$ is flexible due to the rotation of the O=P–O bond compared to the four-membered ring for $[M(Me_2PS_2)_3]^0$. However, we think that this molecular geometry is valid, because the high octahedral symmetry of MO_6 coordination explains the experimental results by UV–vis spectroscopy.[5] Comparing the bond lengths between M (Eu or Am) and the donor atoms of ligands, we found that Am complexes have longer M–O lengths and the same or shorter M–S and M–N lengths than Eu complexes, correlating with the selectivity of Eu(III)/Am(III) by donors. Considering that the radius of the Am(III) ion is larger than that of the Eu(III) ion by ca. 0.03 Å for the six-coordinate system, we indicate that the secondary contribution, such as the covalent interaction between the metal and the ligands, not only the contribution from the ionic interaction, might cause the shortening of the Am–S and Am–N lengths.

3.2. Complex Formation Energy. Table 2 shows the energy difference based on the complex formation reactions in Scheme 1. As expected from the results of the similar geometries for both Eu and Am complexes, there is hardly any difference in the thermal correction contribution ΔG^{corr} between Eu and Am systems. We define the $\Delta\Delta G$ value as eq 6

$$\Delta\Delta G = \Delta G_{Eu} - \Delta G_{Am} \quad (6)$$

where ΔG_{Eu} and ΔG_{Am} are ΔG for Eu and Am systems, respectively. Positive $\Delta\Delta G$ shows that the ligand favors the Am

Table 1. Metal–Ligand Lengths (Angstroms) in the Calculated Equilibrium Structures

		r_{M-X} (M = lanthanide)				r_{M-X} (M = minor actinide)			
complexes		calcd		exp		calcd		exp	
$M(H_2O)_9$	M–O(trigonal)	M = Eu	2.497(7)	M = Eu	2.408[a]	M = Am	2.532(15)	M = Am	2.465[e]
	M–O(tricapped)		2.543(18)		2.536[a]		2.564(27)		2.578[e]
$M(Me_2PS_2)_3$	M–S	M = Eu	2.844(3)	M = Sm	2.788,[b] 2.803[c]	M = Am	2.839(2)	M = Cm	2.826[c]
	M–P		3.401(3)		3.346,[b] 3.40[c]		3.388(2)		3.45[c]
$M(TPEN)(H_2O)_2$	M–N(amine)	M = Eu	2.644(1)	M = Eu	2.614[d]	M = Am	2.630(2)		
	M–N(pyridine)		2.587(47)		2.592[d]		2.587(54)		
	M–O		2.542(3)				2.589(5)		
$M\{(Me_2PO_2)_2H\}_3$	M–O	M = Eu	2.316(21)	M = Sm	2.301[c]	M = Am	2.354(17)	M = Cm	2.320[c]
	M–P		3.684(35)		3.83[c]		2.748(33)		

[a]Reference 22. [b]Reference 24. [c]Reference 5. [d]Reference 25. [e]Reference 23.

DOI: 10.1021/acs.inorgchem.5b01204
Inorg. Chem. 2015, 54, 7103–7109

Table 2. ΔE^{tot} and ΔG^{corr} for Eu/Am Complexes and $\Delta\Delta G$ under Gas- or Water-Phase Conditions (kJ mol^{-1})

		$M(Me_2PS_2)_3$		$M(TPEN)(H_2O)_2$		$M\{(Me_2PO_2)_2H\}_3$	
energy	method	M = Eu	M = Am	M = Eu	M = Am	M = Eu	M = Am
ΔE^{tot}_{gas}	BP86	−2044.8	−2031.6	−277.6	−265.1	−2143.3	−2126.2
	B3LYP	−1952.1	−1953.8	−221.0	−220.3	−2134.8	−2116.4
	B2PLYP	−1930.8	−1955.2	−224.5	−231.5	−2127.0	−2110.0
ΔE^{tot}_{water}	BP86	−123.6	−116.7	−81.5	−76.4	−240.4	−229.8
	B3LYP	−35.3	−43.4	−33.6	−38.3	−227.5	−215.6
	B2PLYP	−20.8	−51.3	−39.5	−50.7	−228.3	−217.5
ΔG^{corr}	BP86	−254.4	−253.4	−273.6	−274.2	−266.1	−262.4
$\Delta\Delta G_{gas}$	BP86	−14.3		−11.8		−20.8	
	B3LYP	0.8		−0.1		−22.1	
	B2PLYP	23.5		7.6		−20.9	
$\Delta\Delta G_{water}$	BP86	−7.8		−4.4		−14.3	
	B3LYP	7.2		5.4		−15.7	
	B2PLYP	29.5		11.8		−14.5	
$\Delta\Delta G$	exp.	21.5[a]		11.4[a]		−7.1[a]	

[a]These values were calculated by using the equation $\Delta\Delta G = RT\ln(D_{Am}/D_{Eu})$ at 298.15 K based on the separation factor given in Figure 1.

Table 3. Comparison of Spin Population of *M* Among BP86, B3LYP, and B2PLYP Functionals

	$\rho^{spin}{}_M$/electron (Eu/Am)			
method	$M(H_2O)_9$	$M(Me_2PS_2)_3$	$M(TPEN)(H_2O)_2$	$M\{(Me_2PO_2)_2H\}_3$
BP86	6.151/6.062	6.492/6.291	6.356/6.217	6.137/6.060
B3LYP	6.033/6.020	6.294/6.155	6.132/6.103	6.045/6.015
B2PLYP	6.032/6.026	6.110/6.111	6.082/6.089	6.037/6.022

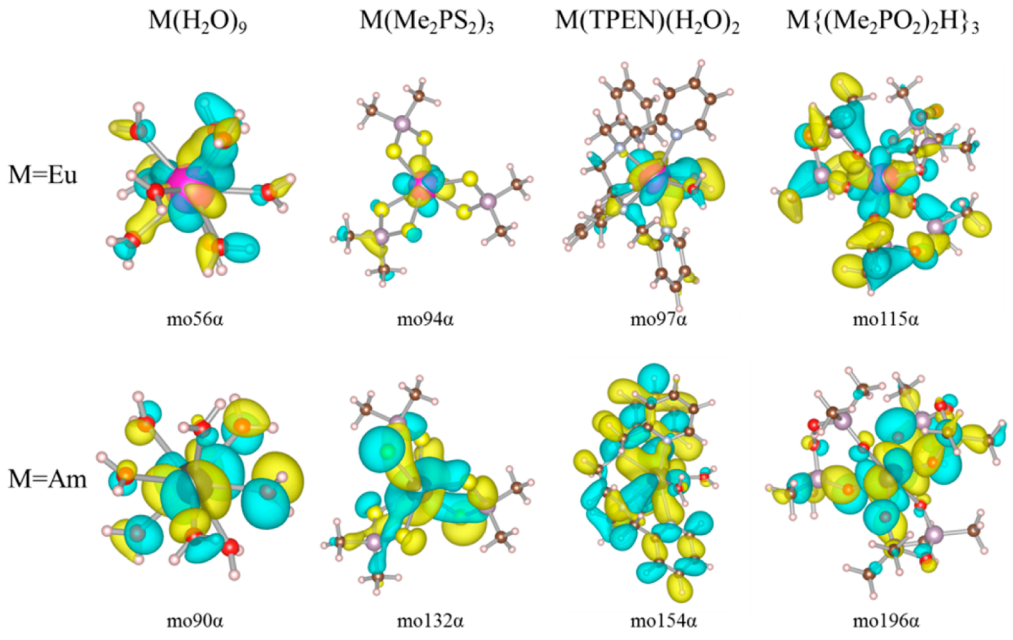

Figure 3. Three-dimensional descriptions of orbital spinors at the B2PLYP level.

ion, whereas negative $\Delta\Delta G$ shows that the ligand favors the Eu ion. Focusing on the sign of the $\Delta\Delta G$ values, we found that the results of B2PLYP for both gas and water phases and B3LYP for water phase reproduce the experimental selectivity of Eu(III)/Am(III) ions by S, N, and O donors. In particular, B2PLYP results show an extremely strong correlation with experiment, because the typical errors of $\Delta\Delta G$ are smaller than a few kJ mol^{-1}. We already indicated that the reproducibility of ^{151}Eu and ^{237}Np Mössbauer isomer shifts is improved in the order BP86, B3LYP, and B2PLYP.[17] The present result suggests that the density functional which could estimate accurately the bonding property for f-block compounds reproduces not only the selectivity on Eu(III)/Am(III) but also the extraction ability for Cyanex301 and TPEN ligands. It might be indicated that the Hartree−Fock exchange admixture of 53% in the B2PLYP functional is a proper fraction to describe the bonding nature for Ln and MA compounds. Furthermore, considering that $\Delta\Delta G_{water}$ is systematically smaller than $\Delta\Delta G_{gas}$ by 4−7 kJ mol^{-1} in the same functional, it is indicated that the COSMO solvation is the minor

DOI: 10.1021/acs.inorgchem.5b01204
Inorg. Chem. 2015, 54, 7103−7109

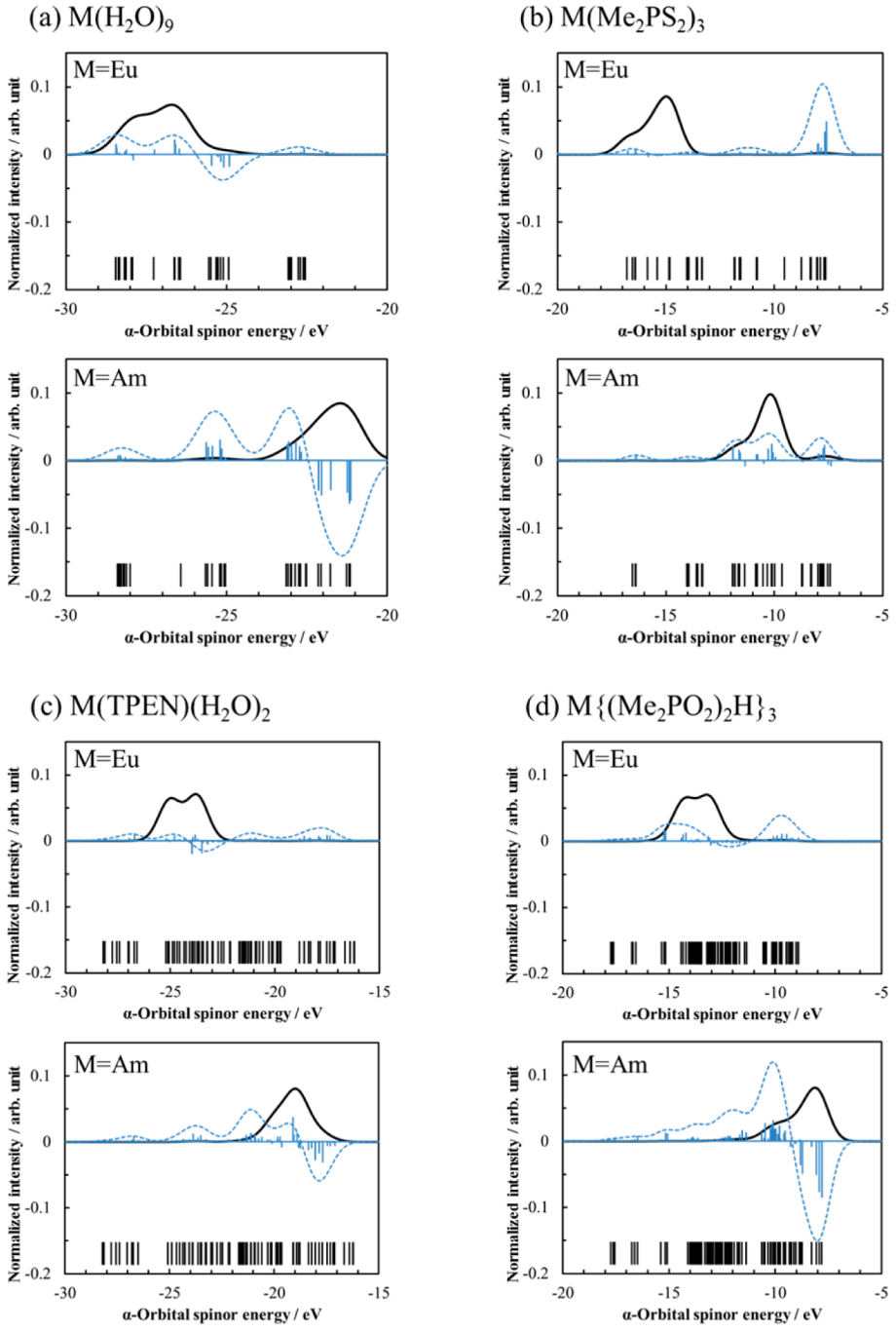

Figure 4. Partial density of states of the metal f orbital and bond overlap population between the metal f orbital and the donor atoms plotted as a black solid line and blue broken line, respectively, for (a) $[M(H_2O)_9]^{3+}$, (b) $[M(Me_2PS_2)_3]^0$, (c) $[M(TPEN)(H_2O)_2]^{3+}$, and (d) $[M\{(Me_2PO_2)_2H\}_3]^0$.

contribution compared to the dependence on density functionals by ~40 kJ mol^{-1}.

3.3. Population Analysis. We focus on Mulliken's spin population of the center metal ($\rho^{spin}{}_M$) in the complexes obtained in the gas phase, because it was indicated that $\rho^{spin}{}_M$ is the important parameter to evaluate the bonding property for f-block complexes.[17] As shown in Table 3, $\rho^{spin}{}_M$ values decrease in the order BP86, B3LYP, and B2PLYP for both Eu and Am complexes. When $\rho^{spin}{}_M$ deviates more from 6.00 electrons, the bonding interaction between the metal and the ligands becomes more covalent, indicating that BP86 and B3LYP methods tend to overestimate the covalency of f-block compounds. Comparing the $\rho^{spin}{}_M$ values between Eu and Am complexes, we found that BP86 and B3LYP functionals give larger $\rho^{spin}{}_M$ values of Eu complexes than those of Am complexes. However, the B2PLYP functional gives larger $\rho^{spin}{}_M$ values of $Eu(H_2O)_9$ and $Eu\{(Me_2PO_2)_2H\}_3$ whereas smaller $\rho^{spin}{}_M$ values of $[Eu(Me_2PS_2)_3]^0$ and $[Eu(TPEN)(H_2O)_2]^{3+}$ compared to those of Am complexes. These results might suggest that the selectivity of the metal ion is determined by the difference in the covalency between Eu and Am complexes from the viewpoint of the reproducibility of the B2PLYP functional.

Here we discuss the bonding nature of Eu and Am complexes at only the B2PLYP level to understand the origin of selectivity

DOI: 10.1021/acs.inorgchem.5b01204
Inorg. Chem. 2015, 54, 7103−7109

for Eu(III)/Am(III) ions. The spin population values $\rho^{spin}{}_{M}$ as an indicator of the covalency consist of the f orbital in the metal and s and p orbitals in the donor atoms. Figure 3 shows the selected α-orbital spinors, which include the population of the metal f orbital, in the valence region. Focused on the bonding between the metal and the donor atoms for $M(H_2O)_9$ and $M\{(Me_2PO_2)_2H\}_3$, bond overlap for the Eu−O bond whereas antibonding overlap for Am−O bond are observed. For $M(Me_2PS_2)_3$ and $M(TPEN)(H_2O)_2$, the nonbonding nature for Eu−S and Eu−N bonds but bond overlap for Am−S and Am−N bonds are observed. Other orbital spinors including f-orbital population are also shown in the Supporting Information. These orbital spinors have bonding nature as mentioned above. This result indicates that the valence f orbital of the metal recognizes the donor atoms and participates in the bonding whose types depend on the donor atoms.

Furthermore, we performed a bond overlap population analysis for quantitative discussion about the bonding properties. We calculated the overlap population between the f orbital of the metal and the s,p orbital of the donor atoms in the region where there are six numbers of the f orbital in the metal occupied. Figure 4 shows the partial density of states (PDOS) of the f orbital and bond overlap population (BOP) to each α-orbital spinor described as the black solid line and blue broken line, respectively. Focused on the region where the f orbital is distributed for $M(H_2O)_9$, the Eu complex has a positive BOP corresponding to a bonding-type contribution, whereas the Am complex has a negative BOP corresponding to an antibonding-type contribution. For $M(Me_2PS_2)_3$, the Eu complex has no distribution of BOP in the f-orbital region, whereas the Am complex has a bonding contribution. For $M(TPEN)(H_2O)_2$, the Eu complex has almost no contribution to the bonding, but the Am complex has bonding and antibonding contributions attributed to Am−N and Am−O interactions, respectively. For $M\{(Me_2PO_2)_2H\}_3$, a similar contribution to $M(H_2O)_9$ was observed. These results are summarized in Table 4. We consider the f-orbital contribution

Table 4. Bonding Types of the Metal f Orbital Depending on Donor Atoms

metal	O donor	N donor	S donor
Eu(III)	weak bonding	nonbonding	nonbonding
Am(III)	strong antibonding	bonding	bonding

of the Am ion to the bonding in the change from $Am(H_2O)_9$ to each donor complex, because the f-orbital contribution of the Eu ion does not significantly change among O, N, and S donors. For $Am(Me_2PS_2)_3$ and $Am(TPEN)(H_2O)_2$, due to the change from "strong anti-bonding" to "bonding", the covalency increases to give the selectivity of the Am ion. Moreover, because $Am(TPEN)(H_2O)_2$ includes an Am−O bond with strong antibonding property, it might be suggested that $Am(Me_2PS_2)_3$ has relatively more covalent interaction, resulting in the higher separation performance of $Me_2PS_2^-$ ($\Delta\Delta G_{gas}$ = 23.5 kJ mol^{-1}) than that of TPEN ($\Delta\Delta G_{gas}$ = 7.6 kJ mol^{-1}). For $M\{(Me_2PO_2)_2H\}_3$, because the donor atoms which coordinate to metal are unchanged, the selectivity of the metal ion is determined by only ionic interaction, leading to the Eu(III) selectivity. In this study, we first revealed that the degree and type of the contribution of the f orbital to the bonding are different between the metal ion and the donor atoms, resulting in the selectivity of Eu(III)/Am(III) ions.

4. CONCLUSION

In the present study, we performed a separation study on Eu(III)/Am(III) ions with S-, N-, and O-donor ligands by means of scalar-relativistic ZORA-DFT calculation. We considered the complex formation reactions in which the chemical components and geometries were experimentally confirmed. The equilibrium structures at the ZORA-BP86/SARC level were consistent with the experimental structures. As per the results of the single-point calculations by BP86, B3LYP, and B2PLYP functionals, the reproducibility of the selectivity of Eu(III)/Am(III) increased in the order BP86, B3LYP, and B2PLYP functionals; in particular, the B2PLYP functional also reproduced the absolute values of $\Delta\Delta G$. This tendency of the reproducibility was consistent with that of ^{151}Eu and ^{237}Np Mössbauer isomer shifts,[17] indicating that the method which can describe the accurate bonding nature in compounds is required to reproduce the experimental selectivity of Eu(III)/Am(III). The results of Mulliken's spin population suggested that BP86 and B3LYP overestimated the covalency in the bonding of Eu−ligand compared to that of Am−ligand, leading to the inconsistency of $\Delta\Delta G$. Bond overlap population analysis at the B2PLYP level revealed that the bonding property between the f orbital of Eu and the donor atoms was basically ionic, whereas the strong covalent interaction was observed in the f orbital of Am. Furthermore, the bonding types of the Am f orbital were "bonding" in S- and N-donor complexes but "anti-bonding" in the O-donor complex, resulting in the difference in whether donor atoms favor the Am ion or not. We first explained comprehensively the origin of the Eu(III)/Am(III) selectivity by the difference in the contribution of the f electron to the bonding between the metal and the donor atoms. It might be expected that our calculation procedure contributes to the prediction of Eu(III)/Am(III) selectivity and the improvement of the separation materials based on the chemical bonding properties between the f orbital and the ligands by the molecular modification and/or element strategy. We believe that the present study sheds light on not only the fundamental f-block chemistry but also the application to the disposal problem of HLLW.

■ ASSOCIATED CONTENT

Supporting Information

Optimized Cartesian atomic coordinates (given as xyz file format), MO description for Eu and Am complexes, and data of energies ($E^{tot}{}_{gas}$, $E^{tot}{}_{water}$, H^{corr}, S, and G^{corr}) for all species. The Supporting Information is available free of charge on the ACS Publications website at DOI: 10.1021/acs.inorgchem.5b01204.

■ AUTHOR INFORMATION

Corresponding Author

*E-mail: snaka@hiroshima-u.ac.jp.

Notes

The authors declare no competing financial interest.

■ REFERENCES

(1) Nash, K. L. *Solvent Extr. Ion Exch.* **1993**, *11*, 729.
(2) Zhu, Y.; Chen, Y.; Jiao, R. *Sovent Extr. Ion Exch.* **1996**, *14*, 61−68.
(3) Watanabe, M.; Mirvaliev, R.; Tachimori, S.; Takeshita, K.; Nakano, Y.; Morikawa, K.; Mori, R. *Chem. Lett.* **2002**, *12*, 1230−1231.
(4) Jensen, M. P.; Bond, A. H. *Radiochim. Acta* **2002**, *90*, 205−209.
(5) Jensen, M. P.; Bond, A. H. *J. Am. Chem. .Soc.* **2002**, *124*, 9870−9877.

DOI: 10.1021/acs.inorgchem.5b01204
Inorg. Chem. 2015, 54, 7103−7109

(6) Jensen, M. P.; Morss, L. R.; Beitz, J. V.; Ensor, D. D. *J. Alloys Compd.* **2000**, *303*−*304*, 137−141.
(7) Kaltsoyannis, N. *Chem. Soc. Rev.* **2003**, *32*, 9−16.
(8) Platas-Iglesias, C.; Roca-Sabio, A.; Regueiro-Figueroa, M.; Esteban-Gomez, D.; de Blas, A.; Rodríguez-Blas, T. *Curr. Inorg. Chem.* **2011**, *1*, 91−116.
(9) Lan, J.; Shi, W.; Yuan, L.; Li, J.; Zhao, Y.; Chai, Z. *Coord. Chem. Rev.* **2012**, *256*, 1406−1417.
(10) Cao, X.; Heidelberg, D.; Ciupka, J.; Dolg, M. *Inorg. Chem.* **2010**, *49*, 10307−10315.
(11) Bhattacharyya, A.; Ghanty, T. K.; Mohapatra, P. K.; Manchanda, V. K. *Inorg. Chem.* **2011**, *50*, 3913−3921.
(12) Keith, J. M.; Batista, E. R. *Inorg. Chem.* **2012**, *51*, 13−15.
(13) Narbutt, J.; Oziminski, W. P. *Dalton Trans.* **2012**, *41*, 14416−14424.
(14) Kirker, I.; Kaltsoyannis, N. *Dalton Trans.* **2011**, *40*, 124−131.
(15) Kaltsoyannis, N. *Inorg. Chem.* **2013**, *52*, 3407−3413.
(16) Jensen, M. P.; Chiarizia, R.; Shkrob, I. A.; Ulicki, J. S.; Spindler, B. D.; Murphy, D. J.; Hossain, M.; Roca-Sabio, A.; Platas-Iglesias, C.; de Blas, A.; Rodríguez-Blas, T. *Inorg. Chem.* **2014**, *53*, 6003−6012.
(17) Kaneko, M.; Miyashita, S.; Nakashima, S. *Dalton Trans.* **2015**, *44*, 8080−8088.
(18) David, F. *J. Less-Common Met.* **1986**, *121*, 27−42.
(19) David, F.; Vokhmin, V.; Ionova, G. *J. Mol. Liq.* **2001**, *90*, 45−62.
(20) Choppin, G. R.; Peterman, D. R. *Coord. Chem. Rev.* **1998**, *174*, 283−299.
(21) David, F.; Vokhmin, V. *New J. Chem.* **2003**, *27*, 1627−1632.
(22) Chatterjee, S.; Maslen, E. N.; Watson, K. J. *Acta Crystallogr., Sect. B* **1988**, *44*, 381−386.
(23) Lindqvist-Reis, P.; Apostolidis, C.; Rebizant, J.; Morgenstern, A.; Klenze, R.; Walter, O.; Fanghänel, T.; Haire, R. G. *Angew. Chem., Int. Ed.* **2007**, *46*, 919−922.
(24) Meseri, Y.; Pinkerton, A. A.; Chapuis, G. *J. Chem. Soc., Dalton Trans.* **1977**, 725−729.
(25) Hazama, R.; Umakoshi, K.; Kabuto, C.; Kabuto, K.; Sasaki, Y. *Chem. Commun.* **1996**, 15−16.
(26) Neese, F. *ORCA*, ver. 3.0.0; Max Planck Institute for Chemical Energy Conversion: Ruhr, Germany, 2013.
(27) van Wüllen, C. *J. Chem. Phys.* **1998**, *109*, 392−399.
(28) Pantazis, D. A.; Neese, F. *J. Chem. Theory Comput.* **2009**, *5*, 2229−2238.
(29) Pantazis, D. A.; Neese, F. *J. Chem. Theory Comput.* **2011**, *7*, 677−684.
(30) Pantazis, D. A.; Chen, X.; Landis, C. R.; Neese, F. *J. Chem. Theory Comput.* **2008**, *4*, 908−919.
(31) Ciupka, J.; Cao, X.; Wiebke, J.; Dolg, M. *Phys. Chem. Chem. Phys.* **2010**, *12*, 13215−13223.
(32) Wiebke, J.; Moritz, A.; Cao, X.; Dolg, M. *Phys. Chem. Chem. Phys.* **2007**, *9*, 459−465.
(33) Neese, F. *J. Comput. Chem.* **2003**, *35*, 1740−1747.
(34) Neese, F.; Wennmofs, F.; Hansen, A.; Becker, U. *Chem. Phys.* **2009**, *356*, 98−109.
(35) Mulliken, R. S. *J. Chem. Phys.* **1955**, *23*, 1833−1840.
(36) Mulliken, R. S. *J. Chem. Phys.* **1955**, *23*, 2338−2342.
(37) Momma, K.; Izumi, F. *J. Appl. Crystallogr.* **2008**, *41*, 653−658.

DOI: 10.1021/acs.inorgchem.5b01204
Inorg. Chem. 2015, 54, 7103−7109